Deformation of carbon nanotubes by surface van der Waals forces

Tobias Hertel, Robert E. Walkup, and Phaedon Avouris*
IBM Research Division, Thomas J. Watson Research Center, Yorktown Heights, New York 10598
(Received 12 February 1998; revised manuscript received 7 May 1998)

The strength and effect of surface van der Waals forces on the shape of multiwalled and single-walled carbon nanotubes is investigated using atomic-force microscopy, continuum mechanics, and molecular-mechanics simulations. Our calculations show that depending on the tube diameter and number of shells, the van der Waals interaction between nanotubes and a substrate results in high binding energies, which has also been determined experimentally. Nanotubes on a substrate may consequently experience radial and axial deformations, which significantly modify the idealized geometry of free nanotubes. These findings have implications for electronic transport and the tribological properties of adsorbed nanotubes.
[S0163-1829(98)05744-0]

In the past few years carbon nanotubes have attracted growing interest due to their exceptional mechanical and electrical properties. Their high-tensile strength, flexural rigidity, and high-aspect ratio make them potentially interesting materials for strong fibers[1–3] and tips in scanning-probe microscopy.[4,5] The electrical properties which, depending on the diameter and helicity of the nanotubes,[6] can be either metallic or semiconducting, also make them candidates for nanowires[7–11] and electronic devices.[12–15] However, the fabrication of carbon-nanotube/metal connections so as to establish electrical contact to the outside world and to perform electrical measurements remains a major challenge. The character (Ohmic or Schottky type) and ''quality'' of nanotube substrate junctions depends upon the geometry of the contact region, which depends on the nanotube substrate interaction. Electronic transport through carbon nanotubes is generally discussed in terms of the idealized geometry of free nanotubes, unperturbed by interaction with the environment. Experimental studies, however, are mostly performed using nanotubes that are dispersed on a substrate with which they therefore interact. Here we investigate the consequences that this interaction can have on the geometric structure of carbon nanotubes using atomic-force microscopy and molecular-mechanics simulations. Even though nanotubes only interact through van der Waals forces with the substrate, the resulting elastic deformations are substantial. We find that the extent of the observed axial and radial elastic deformations depends on the nanotube diameter and number of tube shells. Radial deformations of carbon nanotubes have been studied previously only in nanotube bundles or when free tubes with thin shells and large diameters collapse.[16–18] Finally, the effects the elastic deformations may have on the properties of carbon nanotubes are discussed.

The multiwalled carbon nanotubes used in our experimental studies were dissolved in methylene chloride using an ultrasonic bath to agitate the solution. Once dispersed on a H passivated Si(100) surface, nanotubes could be imaged in air with an atomic force microscope operating in the noncontact mode (M5, Park Scientific Instruments). The commercial tips (Park Scientific Instruments) used for noncontact imaging in our experiments had relatively low-force constants of 0.16–0.24 N/m and resonance frequencies near 25–30 kHz. Molecular-mechanics calculations were performed with the Tinker program employing the MM3 force field.[19–22] Parameters based on alkene species were used to describe the interatomic interactions within the carbon nanotubes. These were found to accurately reproduce the C_{11} and C_{33} elastic constants of nanotubes.[23] The surface van der Waals interaction parameters were obtained by summing atomic van der Waals interactions for an sp^2 hybridized carbon atom interacting with a graphite slab. Energy minimization was based on a Newton method.[22] Tube-surface binding energies and geometries were found to converge rapidly with tube length.

The atomic-force microscopy (AFM) image of a surface region densely covered with nanotubes, most of which are straight and undeformed, is reproduced in Fig. 1(a). A closer look at such images reveals that nanotubes that cross surface features such as other tubes are not entirely straight, but bend and deform elastically [see Fig. 1(b)]. The strain energy that thereby builds up in the tubes is compensated by a gain in binding energy as the tubes maximize their contact area with the substrate. Profiles like the one in Fig. 1(c) can actually be used as unique probes of the nanotube-surface binding energy, provided the Young's modulus of the tubes is known.[24] The total energy of the system can be written as an integral of the strain energy $u(c)$ and the adhesion energy over the entire tube profile:

$$E = \int [u(c) + V(z)]dx, \tag{1}$$

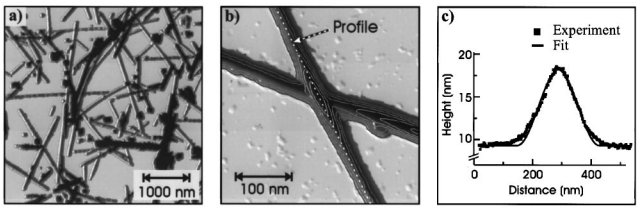

FIG. 1. Multiwalled carbon nanotubes on an H-passivated Si(100) substrate imaged with the AFM. When nanotubes cross obstacles such as other tubes on the surface they bend and deform elastically, as shown in panel (b). Profiles like the one in panel (c) for a nanotube with 90 Å diameter can be used to determine the binding energy of nanotubes to the substrate.

with $c(x)$ being the local-tube curvature and $V(z(x))$ the nanotube-substrate interaction potential at a distance z above the surface (in eV/Å). The interaction potential V may depend on short-ranged chemical and long-ranged van der Waals interactions. However, the shape of profiles calculated from Eq. (1) was found to depend only on the depth and not the particular form of the interaction potential.[24]

From a fit of calculated profiles to the experimental profile of a 90 Å-diameter tube in Fig. 1(c), for example, we obtain a binding energy of ≈ 1.0 eV/Å. The average value for the binding energy of tubes with approximately 95 Å diameter was obtained from about a dozen such profiles and is 0.8 ± 0.3 eV/Å. Compared to smaller molecules interacting with surfaces, these binding energies are high but can be attributed entirely to van der Waals interactions as we discuss later on. As a consequence of these large binding energies, the forces between nanotubes and perturbing features such as defects, steps, or other nanotubes on the surface can be extremely high. Using Eq. (1) to calculate the force with which a 100 Å-diameter tube is pressed against an obstacle of similar height, we obtain a value of 35 nN. We have previously reported that direct evidence for such high forces can be found in profiles along crossing tubes, which clearly show a compression of the lower tube in the contact region.[24] We also find that the total height at the top of such profiles as in Fig. 1(c) is occasionally up to 30% smaller than the sum of the two individual tube heights. This suggests that one or both of the tubes may be compressed at the crossing point. However, unlike the obvious axial deformations discussed above, the AFM is not ideally suited to investigate cross-sectional deformations of nanotubes. We have shown previously that only in extreme cases—when tubes are collapsed entirely—may the AFM, be used to study their structure.[24] The effect of such a compression on the measured nanotube profiles along the tubes axis can safely be neglected. In principle, van der Waals interaction potentials, and thus the force gradients measured in noncontact AFM do depend on the shape of the interacting objects, e.g., the shape of the tip and tube. But even for fundamentally different objects interacting with a surface such as a sphere or cylinder, for example, the observed change in force gradients should be small with a pronounced distance dependence of z^{-3} and $z^{-3.5}$, respectively. Since height differences along the axis of crossing nanotubes are of the order of 100 Å, we conclude that small variations of the tube diameter along such profiles will not have a significant effect on the measured topography, i.e., force gradient images should match the tube topography.

To explore radial and axial deformations in more detail we have, therefore, performed molecular-mechanics calculations on single and multiwalled carbon nanotubes. The results of calculations on isolated nanotubes shown in Fig. 2(a) indicate that the extent of the cross-sectional deformation increases dramatically with increasing tube diameter. This trend can be reversed, however, if inner shells are added to the nanotube [see Fig. 2(b)]. The driving force behind these elastic deformations is provided by the gain in binding energy as the contact area with the substrate increases. The addition of more shells inside a tube increases its rigidity, makes these elastic deformations energetically more costly and, therefore, reduces the observed flattening of the tube wall in contact with the substrate. Such a decrease or increase of the tube's contact area with the substrate should have consequences for the tribological properties of adsorbed nanotubes. The computed binding energies for both, optimized single and multiwalled nanotube geometries reproduce these trends and are summarized in Fig. 3. The open squares give the binding energies obtained for the optimized geometries based on the MM3 force field. The lower boundary of the gray area gives the van der Waals binding energy of a perfectly circular tube, i.e., when no elastic deformations are allowed. The results in Fig. 3 clearly indicate that the net gain in adhesion energy as a consequence of elastic deformations can easily reach 100%. The upper boundary of the gray area gives the van der Waals contribution to the binding energy. The difference between the latter and the binding energies for the optimized geometries thus reflects the strain energy that develops within the tube due to bond bending and bond stretching. When the number of inner shells increases, as illustrated for the (40,40) tube, the cost for elastic deformation cannot be compensated as much by the gain in adhesion energy that results in a smaller flattening of the tube and a lower binding energy. Eventually the binding energy for the solid tube with eight shells is very close to that of a solid tube with no elastic deformation at all. The binding energy for a solid tube thus gives a *lower bound* to the expected adhesion energy. This dependence can be approximated by the empirical fit to our calculated binding energies $E_B = (-0.053 + 0.086d)$ eV/Å, where the diameter of the tubes d is expressed in Å. For solid tubes with around 100 Å diameter we calculate a van der Waals binding energy of 0.8 eV/Å, which agrees very well with the experimental value for the passivated silicon surface. This agreement of the calculated van der Waals binding energy to a graphite surface and the measured binding energy to a passivated silicon surface is not all that surprising due to the similarities of Hamaker constants observed for dissimilar media.[25]

The radial distortions may also have an effect on the tubes' bending properties due to the coupling of the cross section to the flexural rigidity $B = YI$ of nanotubes, where Y

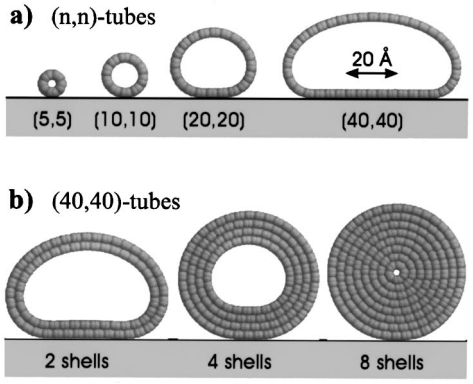

FIG. 2. Radial deformations of adsorbed carbon nanotubes calculated using molecular mechanics. The deformations shown are true representations of the results. (a) The radial compressions of adsorbed single-walled nanotubes with respect to the undistorted free tubes are: 0%, 2%, 13%, and 42%, for 6.7-, 13.5-, 27.1-Å, and 54.2-Å tubes, respectively. (b) When the number of inner shells is increased the compressions are reduced from 42% to 25%, 5% and to less than 1% for (40,40) tubes with 1, 2, 4, and 8 shells, respectively.

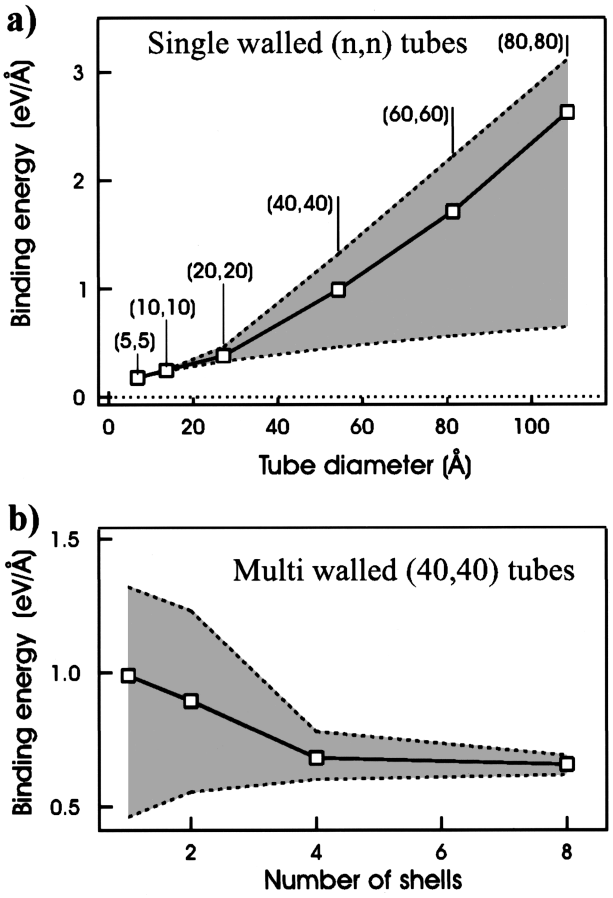

FIG. 3. Binding energies of adsorbed nanotubes as a function of their diameter [panel (a)] or number of inner shells [panel (b)]. Open squares in the middle of the shaded areas give the binding energies as obtained from the molecular-mechanics calculation. The lower side of the shaded areas gives the van der Waals binding energies when no relaxation of the nanotubes is allowed. The upper boundary of the shaded areas gives the van der Waals contribution to the binding energy of the deformed tubes. The difference between this and the results from the MM3 calculation (open squares) thus reflects the cost for elastic deformations.

is Young's modulus and I the geometrical moment of inertia. We may easily estimate the effect of radial distortions on the nanotubes' flexural rigidity if we assume that the compression leads to an elliptical deformation. The change in flexural rigidity for deformed tubes is then calculated from the geometrical moment of inertia $I=\int\int y^2 dx\, dy$ over the cross section of the tube.[26] This estimate reveals that the flexural rigidity of tubes is reduced almost linearly with compression according to $B \cong 1.9 B_0 a/a_0$ where a_0 and a are the outer tube radii for undistorted and elliptically compressed tubes, respectively. Thus, tubes that have undergone significant radial compression can be bent much more easily than perfectly circular tubes.

Adsorbed on a substrate, where nanotubes are likely to encounter obstacles or defects, they will be subject to both radial and axial deformations. We have, therefore, simulated such a situation using molecular mechanics where one tube crosses another one lying on a surface. The results of this optimization for two crossing (10,10) nanotubes with altogether 6800 atoms are reproduced in Fig. 4. These tubes

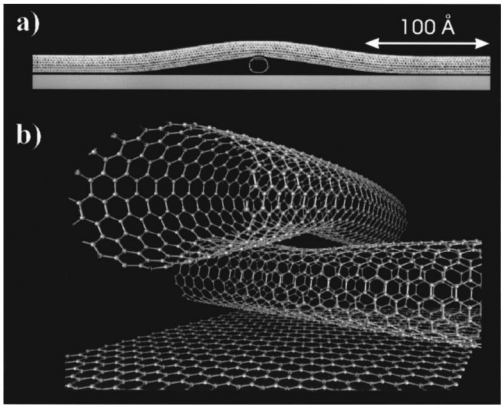

FIG. 4. Results from the molecular-mechanics calculation of two crossing (10,10) nanotubes with axial and radial deformations. Panel (b) gives a perspective closeup of the crossing point. It shows that both tubes are deformed elastically near the contact region. The force acting on the lower tube is about 5 nN.

have a diameter of 13 Å and the longer one has a length of about 350 Å. The axial profile of the upper tube seen in Fig. 4(a) is very similar to the profiles of multiwalled tubes imaged by the AFM [see Fig. 1(c)]. The molecular-mechanics calculations, however, give a more detailed account of the forces and resulting elastic deformations, in particular at the point of contact between the two tubes. We find that the force of 5.5 nN with which the upper tube is pressed against the lower one leads to a cross-sectional compression of both tubes by almost 20% near the point of contact [see Figs. 4(b) and 4(c)]. Further analysis of the molecular mechanics simulations shows that the local strain associated with these deformations can be as high as 5–10 meV per atom. Such strains will lead to a modification of the electronic structure of adsorbed nanotubes and—at small enough temperatures—should have implications for electronic transport properties through nanotubes. Experimental[14] and theoretical[27] studies also indicate a coupling between tube distortions and their electronic transport properties.

Our findings suggest that perturbing features on the surface—such as defects or steps—can induce substantial distortions in adsorbed nanotubes due to their strong adhesion to the substrate. The strain associated with such deformations is very likely the cause for the observed[14] perturbations of the electronic transport properties. This poses a serious challenge for the control required for processing of nanotube devices if they are not to be affected by surface roughness. On the other hand, there is an opportunity to utilize the surface topography as a tool for tailoring the nanotube's transport properties. In this context we have estimated the critical surface roughness—expressed in terms of a critical surface curvature c_c—up to which the tube will smoothly follow the substrate topography. This can be done by calculating the smallest curvature at which the axial strain energy, which develops as the nanotube bends, can still be compensated by the adhesion energy. We found that since the strain energy increases more rapidly with tube diameter d than the adhesion energy ($\propto d^4$ and $\propto d$, respectively) this critical curvature is only about $(12d)^{-1}$ for a tube with 13 Å diameter and decreases to $\approx (50d)^{-1}$ for tube diameters around 100 Å. Thus, a substrate with surface features having a curvature

higher than c_c provides perturbing obstacles that lead to the kind of elastic deformations seen in Fig. 4.

In summary, we found that the van der Waals interaction between nanotubes and a substrate can lead to substantial axial and radial deformations of adsorbed nanotubes destroying the idealized shape of free tubes. This has important implications for tribological and electronic transport properties of adsorbed nanotubes. Experimentally determined adhesion energies for nanotubes bound to a passivated silicon surface could be attributed entirely to van der Waals interactions. The observed flattening of adsorbed nanotubes on the side facing the substrate can lead to a substantial increase in the contact area and binding energy with respect to undeformed tubes. Owing to the linear relationship between contact area and shear forces the larger contact area of deformed tubes allows to stabilize highly strained tube configurations like those observed recently with the AFM.[3,24] In fact, we found that collapsed tubes with the highest possible contact area could not be pushed around on the surface by the tip of an AFM—unlike their inflated ''cousins.''[24] The elastic deformations and the resulting strains that we observe when nanotubes interact with surface features are likely responsible for irregularities in the electronic transport properties of adsorbed nanotubes.[14,27]

We thank H. Dai for providing us with a sample of multiwalled carbon nanotubes. T.H. acknowledges financial support by the Alexander von Humboldt foundation and the Max-Planck-Society.

*Electronic address: avouris@us.ibm.com

[1] M. M. J. Treacy, T. W. Ebbesen, and J. M. Gibson, Nature (London) **381**, 678 (1996).
[2] E. W. Wong, P. E. Sheehan, and C. M. Lieber, Science **277**, 1971 (1997).
[3] M. R. Falvo, G. J. Clary, R. M. T. Il, V. Chi, F. P. Brooks, S. Washburn, and R. Superfine, Nature (London) **389**, 582 (1997).
[4] H. Dai, E. W. Wong, and C. M. Lieber, Nature (London) **384**, 147 (1996).
[5] S. S. Wong, E. Joselevitch, A. T. Wooley, C. L. Cheung, and C. M. Lieber, Nature (London) **394**, 52 (1998).
[6] R. Saito, M. Fujita, G. Dresselhaus, and M. S. Dresselhaus, Appl. Phys. Lett. **60**, 2204 (1992).
[7] L. Langer, L. Stockman, J. P. Heremans, V. Bayot, C. H. Olk, and J.-P. Ishi, J. Mater. Res. **9**, 927 (1994).
[8] T. W. Ebbesen, H. J. Lezec, H. Hiura, J. W. Bennett, H. F. Gheami, and T. Thio, Nature (London) **382**, 54 (1996).
[9] A. Thess, R. Lee, P. Nikolaev, H. Dai, P. Petit, J. Robert, C. Xu, Y. H. Lee, S. G. Kim, A. Rinzler, D. T. Colbert, G. E. Scuseira, D. Tomanek, J. E. Fischer, and R. E. Smalley, Science **273**, 483 (1996).
[10] M. Bockrath, D. H. Dobden, P. L. McEuen, N. G. Chopra, A. Zettl, A. Thess, and R. E. Smalley, Science **275**, 1922 (1997).
[11] S. J. Tans, A. R. M. Verschueren, and C. Dekker, Nature (London) **386**, 474 (1997).
[12] L. Chico, V. H. Crespi, L. X. Benedict, S. G. Louie, and M. Cohen, Phys. Rev. Lett. **76**, 971 (1996).
[13] R. Saito, G. Dresselhaus, and M. S. Dresselhaus, Phys. Rev. B **53**, 2044 (1996).
[14] A. Bezryadin, A. R. M. Verschueren, S. J. Tans, and C. Dekker, Phys. Rev. Lett. **80**, 4036 (1998).
[15] S. J. Tans, A. R. M. Verschueren, and C. Dekker, Nature (London) **393**, 49 (1998).
[16] R. S. Ruoff, J. Tersoff, D. L. Lorents, S. Subramoney, and B. Chan, Nature (London) **364**, 514 (1993).
[17] J. Tersoff and R. S. Ruoff, Phys. Rev. Lett. **73**, 676 (1994).
[18] N. G. Chopra, L. X. Benedict, V. H. Crespi, M. L. Cohen, S. G. Louie, and A. Zettl, Nature (London) **377**, 135 (1995).
[19] Y. Kong and J. W. Ponder, J. Chem. Phys. **107**, 481 (1997).
[20] C. E. Kundrot, J. W. Ponder, and F. M. Richards, J. Comput. Chem. **12**, 402 (1991).
[21] M. J. Dudek and J. W. Ponder, J. Comput. Chem. **16**, 791 (1995).
[22] J. W. Ponder and F. M. Richards, J. Comput. Chem. **8**, 1016 (1987).
[23] J. P. Lu, Phys. Rev. Lett. **79**, 1297 (1997).
[24] T. Hertel, R. Martel, and Ph. Avouris, J. Phys. Chem. B **102**, 910 (1998).
[25] J. Israelachvili, *Intermolecular & Surface Forces* (Academic, London, 1994).
[26] D. J. Barber and R. Loudon, *An Introduction to the Properties of Condensed Matter* (Cambridge University Press, Cambridge, 1989).
[27] A. Rochefort, D. R. Salahub, and Ph. Avouris, Chem. Phys. Lett. (to be published).